Supplementary Figures:

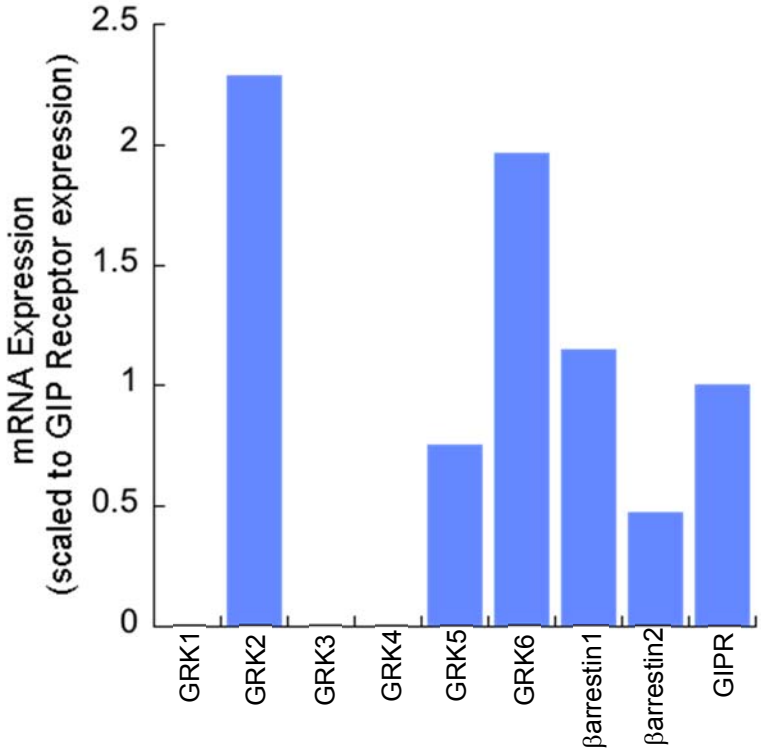

Figure S1. Related to Fig 1 and 2. Expression in 3T3-L1 adipocytes measured by RNAseq reads normalized to the expression of GIPR. Three GRK isoforms, GRK2, 5 and 6 are expressed, and both non visual arrestins, β-arrestins1 and β-arrestins2 are expressed. Expression levels are normalized to mRNA expression of GIP receptor (GIPR).

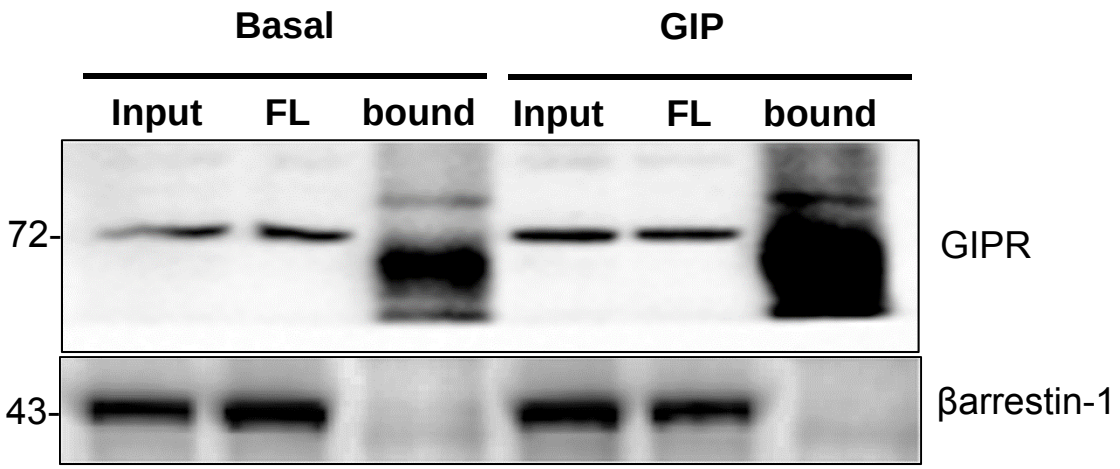

Figure S2. Related to Fig 2. βarrestin-1 does not Co-IP with HA-GIPR GFP in either basal or GIP stimulated adipocytes,

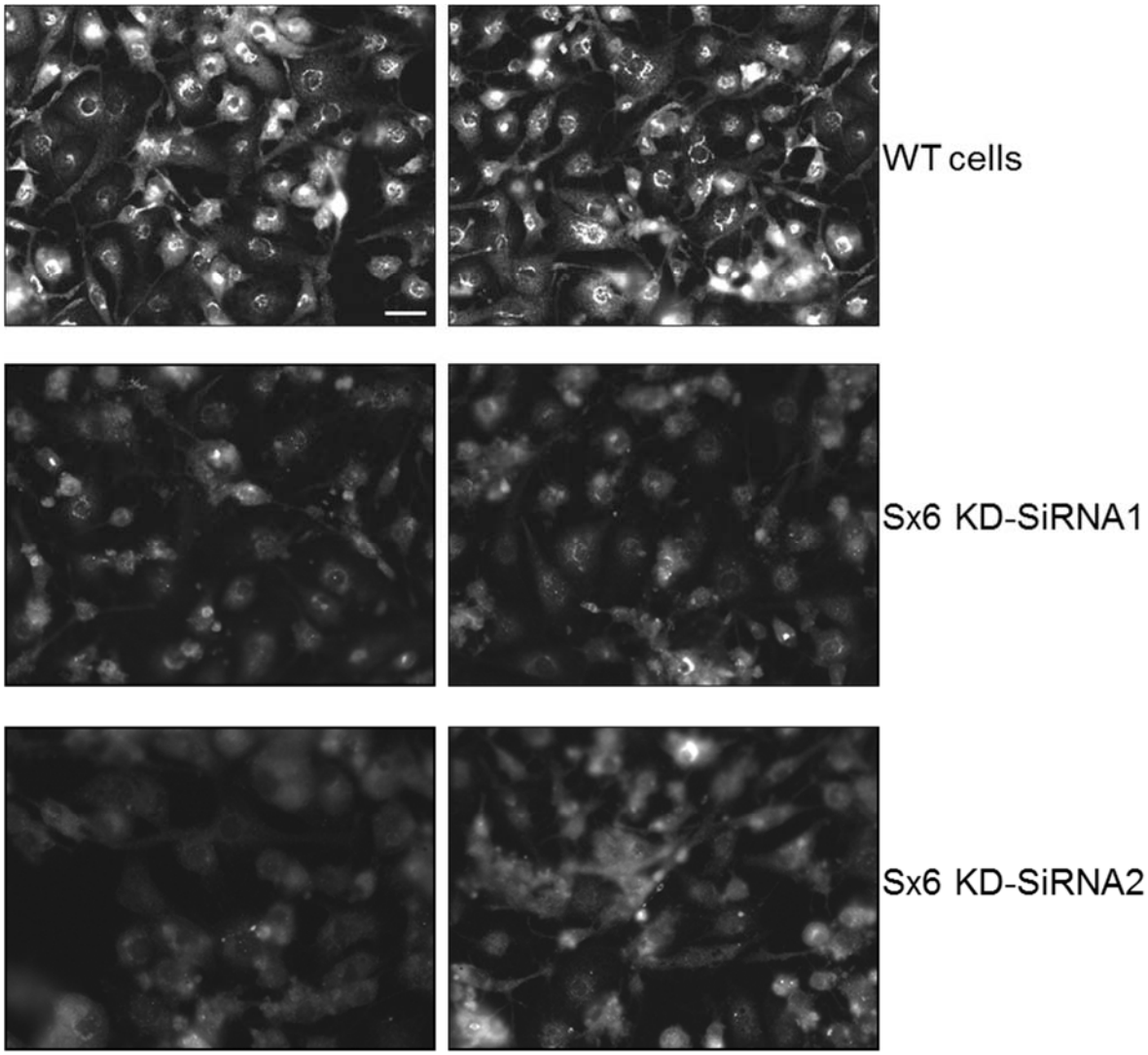

Figure S3. Related To Fig 4. Syntaxin-6 expression in wild type adipocytes and 24 hours post knockdown by two different SiRNAs. Scale bar= 100μm

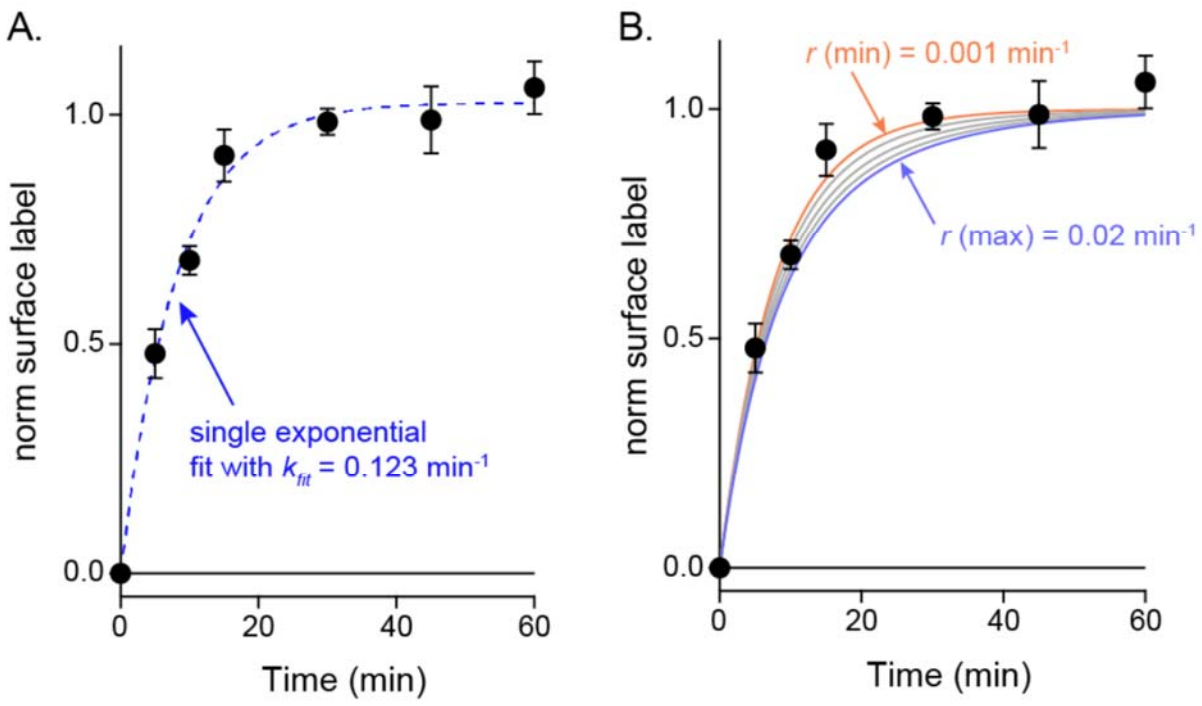

Figure S4. Related to Fig 4. **A.** GIPR exocytosis data in WT adipocytes as shown in Figure 1. Data are fit to a single exponential with fit constant *kfit* as indicated on the graph (*dotted line*). **B.** Same data are fit to **Equation 9** while varying *r* between 0.001 (*orange*) and 0.02 per minute (*blue*). For *r* > 0.02, the recovery curve fell outside of the lower error bars for most of the data, indicating that *r* cannot be greater than 0.02 per minute.

Supplementary Table 1. Related to Fig 1. The beta arrestin knock-down efficiency in 3T3-L1 adipocytes using siRNA.

	Beta arrestin-1	Beta arrestin-2
% knockdown	89±5	65±7

Supplementary Table 2. Related to Fig 2.The knock-down efficiency for different GRKs in 3T3-L1 adipocytes using siRNA.

	GRK-2	GRK-5	GRK-6
% knockdown	87±4	86±6	91±4

Supplementary Methods:

GIPR exocytosis. Cells transiently transfected with HA-GIPR-GFP were incubated in serum free media for 2 hours. Incubated further with or without 100 nM GIP for 60 min. Cells were then incubated with anti HA antibody for times ranging from 5 min to 60 min. 100 nM GIP was included for GIP treatment group. Cells were cooled immediately, fixed and stained with Cy3 secondary after permeabilization. Cell associated anti-HA antibody was quantified as Cy3 fluorescence. Cy3 normalized to GFP (Cy3:GFP) was plotted against time. The data were fit to a single exponential rise to derive an apparent exocytic rate constant.

GIPR internalization. Cells electroporated with HA-GIPR-GFP were starved in serum free media for two hours. Incubated further with or without 100 nM GIP for 60 min. Cells were then incubated in anti-HA antibody with or without GIP for different times from 2 min to 15 min., at the end of each time point, the cells were immediately cooled and fixed. The surface bound antibody was stained with Cy5 secondary in non-permeabilized cells. The internalized antibody was stained with Cy3, after permeabilization. The internalized anti-HA antibody was quantified at each time point as Cy3 fluorescence. Cy3:Cy5 was plotted against time, fitted on the equation for straight line. The slope of the line was calculated as the apparent rate constant of internalization.

Kinetic model derivation and description. We developed a kinetic model to explore the trafficking between the ERC and TGN compartments revealed by the surface labeling experiments described in Fig 1C-E. The model posits three compartments through which GIPR cycles: the plasma membrane (*S*), the ERC (*E*), and the TGN (*T*). Under the experimental conditions used to measure delivery of internal GIPR to the plasma membrane, the rate of internalization has no impact on the rate of surface accumulation. Thus a total of three rate constants are required to describe the cycling from ERC to plasma membrane (k_{ERC}), ERC to TGN (k_{sort}), and TGN to plasma membrane (k_{TGN}) (Scheme 1).

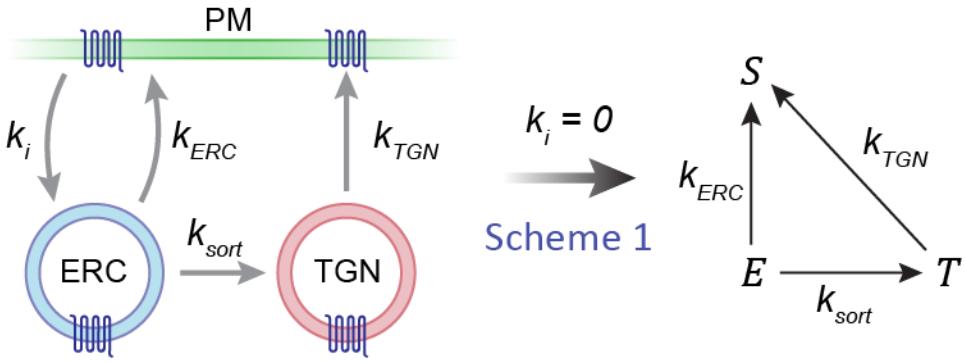

The kinetics of surface accumulation are described by three first-order differential equations:

$$\frac{dE}{dt} = -(k_{sort} + k_{ERC})E(t) \quad (1)$$

$$\frac{dT}{dt} = k_{sort}E(t) - k_{TGN}T(t) \quad (2)$$

$$\frac{dS}{dt} = k_{ERC}E(t) + k_{TGN}T(t) \quad (3)$$

Assuming that the initial number of GIPRs in the ERC, TGN, and plasma membrane are E_0, T_0, and S_0, respectively, these equations were solved to produce analytical expressions for the three compartments as shown in Equations 4-7.

$$E(t) = E_0 e^{-(k_{sort}+k_{ERC})t} \quad (4)$$

$$T(t) = (T_0 + \sigma E_0)e^{-k_{TGN}t} - \sigma E_0 e^{-(k_{sort}+k_{ERC})t}$$

$$E(t) = E_0 e^{-(k_{sort}+k_{ERC})t} \quad (4)$$

$$T(t) = (T_0 + \sigma E_0)e^{-k_{TGN}t} - \sigma E_0 e^{-(k_{sort}+k_{ERC})t} \quad (5)$$

where $\sigma = k_{sort}/(k_{sort} + k_{ERC} - k_{TGN})$ (6)

$$S(t) = S_0 + \frac{E_0(k_{ERC} - \sigma k_{TGN})}{k_{sort}+k_{ERC}}\left(1 - e^{-(k_{sort}+k_{ERC})t}\right) + (T_0 + \sigma E_0)(1 - e^{-k_{TGN}t}) \quad (7)$$

After subtracting the initial surface signal and normalizing to the total internal pool, the recovery function *n(t)* was defined as:

$$n(t) = \frac{S(t)-S_0}{E_0+T_0} = 1 - \left(\frac{(1-\sigma)E_0}{E_0+T_0}\right) \cdot e^{-(k_{sort}+k_{ERC})t} - \left(\frac{T_0+\sigma E_0}{E_0+T_0}\right) \cdot e^{-k_{TGN}t} \quad (8)$$

Note that Equation 8 implies two distinct kinetic components with amplitudes arising from a mixture of both internal compartment populations. The “fast” component represents escape from the ERC to both the TGN and plasma membrane with a rate constant of k_{sort} + k_{ERC}. The slower component is purely the movement of GIPR from the TGN to the plasma membrane with a rate constant of k_{TGN}. The surface labeling experiments were performed under steady-state conditions, so the initial amounts of GIPR in the two internal compartments can be expressed in terms of the rate constants from the full kinetic model presented in Fig 4. Using the steady-state assumption, Equation 8 can be expressed solely in terms of rate constants as follows:

$$n(t) = 1 - A \cdot e^{-(k_{sort}+k_{ERC})t} - (1 - A) \cdot e^{-k_{TGN}t} \quad (9)$$

$$A = \left(\frac{1 - k_{sort}/(k_{sort} + k_{ERC} - k_{TGN})}{k_{sort}/k_{TGN} + 1}\right)$$

(9a)

Based on the observations that internalization of GIPR and surface delivery of the TR and TGN46 were all independent of GIP treatment, the most parsimonious method of incorporating GIP modulation into this kinetic model is to assume that the rate constant for trafficking from the ERC to the TGN (k_{sort}) is the only parameter affected by GIP. Thus, we asked whether there exists a consistent set of kinetic parameters such that the exocytosis kinetics in basal and GIP-treated adipocytes could be entirely explained merely by altering the parameter k_{sort}.

The surface labeling experiments in Figure 4 were fit using Equation 9 with k_{TGN} and k_{sort} as fit parameters. All numerical analysis was performed in Igor Pro (Wavemetrics). Estimated parameters are reported along with ± one standard deviation generated by the fitting software. k_{ERC} was estimated to be 0.123 ± 0.012 per minute by fitting the basal recovery kinetics to a single exponential, because most of the internal GIPR resides in the ERC and traffics directly to the plasma membrane in the absence of GIP (Fig 3A). The TGN→PM rate constant k_{TGN} is further constrained by the steady-state surface fraction (f_S) and rate of internalization (k_i) based on the restriction that all rate constants must be greater than 0:

$$k_{TGN}\, max < k_i f_s/(1 - f_s) \qquad (10)$$

The surface fraction of GIPR decreases upon GIP treatment so this condition sets the upper limit allowed for k_{TGN}. Given a surface fraction of around 45% and an internalization rate constant ranging between 0.07-0.085 per minute, the maximum allowable value of k_{TGN} falls between 0.058 and 0.07 per min. Fits to the surface delivery of GIPR in GIP-treated adipocytes using Equation 9 using data points collected between 5 minutes and 1 hour estimate k_{TGN} to be 0.06 ± 0.0076 per min. By fixing k_{TGN} and k_{ERC} to 0.06 per min and 0.123 per min, respectively, k_{sort} was then estimated in both untreated and GIP treated adipocytes (Figure 4). In control conditions, the numerical fits were not well behaved and k_{sort} could only be estimated within a relatively broad range of small values (0.001 ± 0.004 per min) with an upper bound of 0.02 per min. At rates faster than 0.02 per min, the predicted surface delivery kinetics consistently fell outside the range for most of the measured time points between 5 and 60 minutes (SuppFig 3B). In contrast, k_{sort} could be reasonably well estimated in GIP-treated adipocytes (0.222 ± 0.110 per min). Thus, differences in surface delivery of GIPR could be entirely explained by

increasing the rate constant k_{sort} from 0.001 to 0.222 per minute while leaving all other parameters constant (Figure 4). The fold increase in k_{sort} between control and GIP treated adipocytes

The model presented here also constrains the maximum possible change in surface GIPR given the values estimated for k_{TGN} and k_{ERC}. If k_{sort} is essentially 0, all GIPR trafficking is limited to the ERC and PM and the surface fraction reaches its maximum value based on Scheme 2. In contrast, if k_{sort} is very large so that all GIPR instantaneously moves from the ERC to the TGN, the surface fraction falls to its minimum value based on Scheme 3.

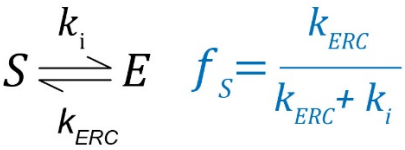

Scheme 2

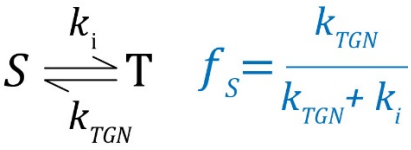

Scheme 3

These two extremes constrain the maximal amount of surface GIPR modulation as given by Equation 11.

Maximum fractional drop in surface GIPR is $= 1 - \left(\frac{k_{TGN}}{k_{ERC}}\right)\frac{k_{ERC} + k_i}{k_{TGN} + k_i}$ (11)

Using the values estimated in this study, the maximum drop in surface GIPR is predicted to be ~30%. This is close to the observed drop in surface GIPR, indicating that the proposed trafficking pathway is maximally modulated by GIP treatment in adipocytes.